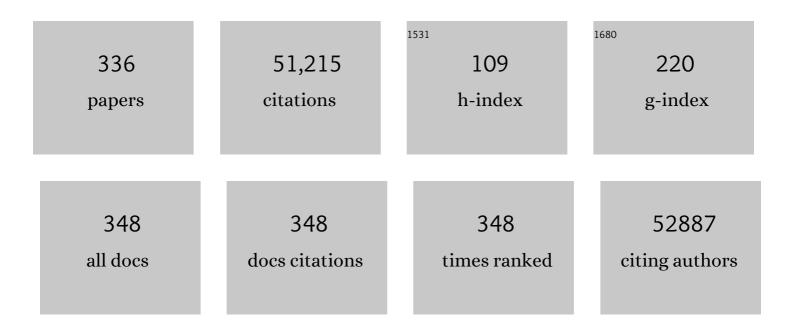
## Xiao-Ming Sun

List of Publications by Year in descending order

Source: https://exaly.com/author-pdf/4230437/publications.pdf Version: 2024-02-01



#	Article	IF	CITATIONS
1	Sandwich layered double hydroxides with graphene oxide for enhanced water desalination. Science China Materials, 2022, 65, 803-810.	3.5	17
2	Single-atom Zn for boosting supercapacitor performance. Nano Research, 2022, 15, 1715-1724.	5.8	26
3	Ultrathin Aluminum Nanosheets Grown on Carbon Nanotubes for High Performance Lithium Ion Batteries. Advanced Functional Materials, 2022, 32, 2109112.	7.8	17
4	Copper nanowire with enriched highâ€index facets for highly selective CO <sub>2</sub> reduction. SmartMat, 2022, 3, 142-150.	6.4	19
5	Surface hydrophobic modification enhanced catalytic performance of electrochemical nitrogen reduction reaction. Nano Research, 2022, 15, 3886-3893.	5.8	40
6	Strong Metal–Support Interaction Boosts Activity, Selectivity, and Stability in Electrosynthesis of H <sub>2</sub> O <sub>2</sub> . Journal of the American Chemical Society, 2022, 144, 2255-2263.	6.6	90
7	SND1 Promotes Radioresistance in Cervical Cancer Cells by Targeting the DNA Damage Response. Cancer Biotherapy and Radiopharmaceuticals, 2022, , .	0.7	1
8	Uncovering sulfur doping effect in MnO2 nanosheets as an efficient cathode for aqueous zinc ion battery. Energy Storage Materials, 2022, 47, 424-433.	9.5	161
9	3D printed hierarchical spinel monolithic catalysts for highly efficient semi-hydrogenation of acetylene. Nano Research, 2022, 15, 6010-6018.	5.8	8
10	Stabilizing single-atomic ruthenium by ferrous ion doped NiFe-LDH towards highly efficient and sustained water oxidation. Chemical Engineering Journal, 2022, 446, 136962.	6.6	25
11	Unraveling the effects of gas species and surface wettability on the morphology of interfacial nanobubbles. Nanoscale Advances, 2022, 4, 2893-2901.	2.2	3
12	Oxygenated P/N co-doped carbon for efficient 2e <sup>â^'</sup> oxygen reduction to H <sub>2</sub> O <sub>2</sub> . Journal of Materials Chemistry A, 2022, 10, 14355-14363.	5.2	22
13	Recycling synthesis of single-atom Zn-nitrogen-carbon catalyst for electrocatalytic reduction of O2 to H2O2. Science China Materials, 2022, 65, 3490-3496.	3.5	10
14	Construction of Dual-Atom Fe via Face-to-Face Assembly of Molecular Phthalocyanine for Superior Oxygen Reduction Reaction. Chemistry of Materials, 2022, 34, 5598-5606.	3.2	29
15	Iridium Doped Pyrochlore Ruthenates for Efficient and Durable Electrocatalytic Oxygen Evolution in Acidic Media. Small, 2022, 18, .	5.2	34
16	Electrochemical Oxygen Reduction to Hydrogen Peroxide via a Twoâ€Electron Transfer Pathway on Carbonâ€Based Singleâ€Atom Catalysts. Advanced Materials Interfaces, 2021, 8, 2001360.	1.9	35
17	Kinetic study of electrochemically produced hydrogen bubbles on Pt electrodes with tailored geometries. Nano Research, 2021, 14, 2154-2159.	5.8	15
18	Layered double hydroxide-based electrocatalysts for the oxygen evolution reaction: identification and tailoring of active sites, and superaerophobic nanoarray electrode assembly. Chemical Society Reviews, 2021, 50, 8790-8817.	18.7	331

#	Article	IF	CITATIONS
19	Oxygen Reduction Reaction: MnN <sub>4</sub> Oxygen Reduction Electrocatalyst: Operando Investigation of Active Sites and High Performance in Zinc–Air Battery (Adv. Energy Mater. 6/2021). Advanced Energy Materials, 2021, 11, 2170025.	10.2	0
20	Rare-earth-regulated Ru-O interaction within the pyrochlore ruthenate for electrocatalytic oxygen evolution in acidic media. Science China Materials, 2021, 64, 1653-1661.	3.5	27
21	Synthesis of Nanosized Metal Sulfides Using Elemental Sulfur in Formamide: Implications for Energy Conversion and Optical Scenarios. ACS Applied Nano Materials, 2021, 4, 2357-2364.	2.4	6
22	Superwetting behaviors at the interface between electrode and electrolyte. Cell Reports Physical Science, 2021, 2, 100374.	2.8	22
23	Dual-atom Pt heterogeneous catalyst with excellent catalytic performances for the selective hydrogenation and epoxidation. Nature Communications, 2021, 12, 3181.	5.8	156
24	Fast and Stable Electrochemical Production of H <sub>2</sub> O <sub>2</sub> by Electrode Architecture Engineering. ACS Sustainable Chemistry and Engineering, 2021, 9, 7120-7129.	3.2	24
25	Aerophilic Co-Embedded N-Doped Carbon Nanotube Arrays as Highly Efficient Cathodes for Aluminum–Air Batteries. ACS Applied Materials & Interfaces, 2021, 13, 26853-26860.	4.0	15
26	Hollow Carbon Spheres Embedded with VN Quantum Dots as an Efficient Cathode Host for Lithium–Sulfur Batteries. Energy & Fuels, 2021, 35, 10219-10226.	2.5	17
27	GILT in tumor cells improves T cell-mediated anti-tumor immune surveillance. Immunology Letters, 2021, 234, 1-12.	1.1	5
28	Energy-saving hydrogen production by chlorine-free hybrid seawater splitting coupling hydrazine degradation. Nature Communications, 2021, 12, 4182.	5.8	233
29	Ultrathin-shell epitaxial Ag@Au core-shell nanowires for high-performance and chemically-stable electronic, optical, and mechanical devices. Nano Research, 2021, 14, 4294-4303.	5.8	35
30	Flexible carbon nanofiber film with diatomic Fe-Co sites for efficient oxygen reduction and evolution reactions in wearable zinc-air batteries. Nano Energy, 2021, 87, 106147.	8.2	103
31	A mixed ion-electron conducting network derived from a porous CoP film for stable lithium metal anodes. Materials Chemistry Frontiers, 2021, 5, 5486-5496.	3.2	7
32	Controllable synthesis and electrocatalytic applications of atomically precise gold nanoclusters. Nanoscale Advances, 2021, 3, 6330-6341.	2.2	14
33	Catalytic separators with Co–N–C nanoreactors for high-performance lithium–sulfur batteries. Inorganic Chemistry Frontiers, 2021, 8, 3066-3076.	3.0	29
34	MnN <sub>4</sub> Oxygen Reduction Electrocatalyst: Operando Investigation of Active Sites and High Performance in Zinc–Air Battery. Advanced Energy Materials, 2021, 11, 2002753.	10.2	83
35	lridium in Tungsten Trioxide Matrix as an Efficient Biâ€Functional Electrocatalyst for Overall Water Splitting in Acidic Media. Small, 2021, 17, e2102078.	5.2	28
36	Research Progress of Oxygen Evolution Reaction Catalysts for Electrochemical Water Splitting. ChemSusChem, 2021, 14, 5359-5383.	3.6	70

#	Article	IF	CITATIONS
37	MoSx microgrid electrodes with geometric jumping effect for enhancing hydrogen evolution efficiency. Science China Materials, 2021, 64, 892-898.	3.5	3
38	The chemistry, recent advancements and activity descriptors for macrocycles based electrocatalysts in oxygen reduction reaction. Coordination Chemistry Reviews, 2020, 402, 213047.	9.5	78
39	Ternary NiCoFe-layered double hydroxide hollow polyhedrons as highly efficient electrocatalysts for oxygen evolution reaction. Journal of Energy Chemistry, 2020, 43, 104-107.	7.1	52
40	Ultra-thin metal-organic framework nanoribbons. National Science Review, 2020, 7, 46-52.	4.6	38
41	A multiphase nickel iron sulfide hybrid electrode for highly active oxygen evolution. Science China Materials, 2020, 63, 356-363.	3.5	23
42	Synthesis and Properties of Stable Sub-2-nm-Thick Aluminum Nanosheets: Oxygen Passivation and Two-Photon Luminescence. CheM, 2020, 6, 448-459.	5.8	15
43	Atomically Dispersed Mo Supported on Metallic Co <sub>9</sub> S <sub>8</sub> Nanoflakes as an Advanced Nobleâ€Metalâ€Free Bifunctional Water Splitting Catalyst Working in Universal pH Conditions. Advanced Energy Materials, 2020, 10, 1903137.	10.2	162
44	An Artificial Electrode/Electrolyte Interface for CO <sub>2</sub> Electroreduction by Cation Surfactant Selfâ€Assembly. Angewandte Chemie - International Edition, 2020, 59, 19095-19101.	7.2	71
45	Electronic coupling strategy to boost water oxidation efficiency based on the modelling of trimetallic hydroxides Ni1-x-yFexCry(OH)2: From theory to experiment. Chemical Engineering Journal, 2020, 402, 126144.	6.6	11
46	An Artificial Electrode/Electrolyte Interface for CO <sub>2</sub> Electroreduction by Cation Surfactant Selfâ€Assembly. Angewandte Chemie, 2020, 132, 19257-19263.	1.6	45
47	Trifunctional Singleâ€Atomic Ru Sites Enable Efficient Overall Water Splitting and Oxygen Reduction in Acidic Media. Small, 2020, 16, e2002888.	5.2	120
48	Thiolâ€Branched Solid Polymer Electrolyte Featuring High Strength, Toughness, and Lithium Ionic Conductivity for Lithiumâ€Metal Batteries. Advanced Materials, 2020, 32, e2001259.	11.1	139
49	Understanding of Dynamic Contacting Behaviors of Underwater Gas Bubbles on Solid Surfaces. Langmuir, 2020, 36, 11422-11428.	1.6	7
50	Antibuoyancy and Unidirectional Gas Evolution by Janus Electrodes with Asymmetric Wettability. ACS Applied Materials & Interfaces, 2020, 12, 23627-23634.	4.0	29
51	Bubble Consumption Dynamics in Electrochemical Oxygen Reduction. Chemical Research in Chinese Universities, 2020, 36, 473-478.	1.3	3
52	Boosting the bifunctional oxygen electrocatalytic performance of atomically dispersed Fe site via atomic Ni neighboring. Applied Catalysis B: Environmental, 2020, 274, 119091.	10.8	130
53	Assisting Atomic Dispersion of Fe in N-Doped Carbon by Aerosil for High-Efficiency Oxygen Reduction. ACS Applied Materials & Interfaces, 2020, 12, 25832-25842.	4.0	17
54	Atomically Dispersed Fe-N4 Modified with Precisely Located S for Highly Efficient Oxygen Reduction. Nano-Micro Letters, 2020, 12, 116.	14.4	99

#	Article	IF	CITATIONS
55	Acid–Base Interaction Enhancing Oxygen Tolerance in Electrocatalytic Carbon Dioxide Reduction. Angewandte Chemie - International Edition, 2020, 59, 10918-10923.	7.2	40
56	Acid–Base Interaction Enhancing Oxygen Tolerance in Electrocatalytic Carbon Dioxide Reduction. Angewandte Chemie, 2020, 132, 11010-11015.	1.6	6
57	A pan-cancer analysis of the oncogenic role of staphylococcal nuclease domain-containing protein 1 (SND1) in human tumors. Genomics, 2020, 112, 3958-3967.	1.3	98
58	Pyrolysis-free formamide-derived N-doped carbon supporting atomically dispersed cobalt as high-performance bifunctional oxygen electrocatalyst. Journal of Energy Chemistry, 2020, 49, 283-290.	7.1	35
59	Insights into the Enhanced Catalytic Activity of Fe-Doped LiCoPO <sub>4</sub> for the Oxygen Evolution Reaction. ACS Applied Energy Materials, 2020, 3, 2959-2965.	2.5	5
60	Hollow-Structured Layered Double Hydroxide: Structure Evolution Induced by Gradient Composition. Inorganic Chemistry, 2020, 59, 1804-1809.	1.9	10
61	Ultrasmall NiFe layered double hydroxide strongly coupled on atomically dispersed FeCo-NC nanoflowers as efficient bifunctional catalyst for rechargeable Zn-air battery. Science China Materials, 2020, 63, 1182-1195.	3.5	44
62	Electroreduction of CO <sub>2</sub> to Formate on a Copper-Based Electrocatalyst at High Pressures with High Energy Conversion Efficiency. Journal of the American Chemical Society, 2020, 142, 7276-7282.	6.6	165
63	Sacrificial carbon nitride-templated hollow FeCo-NC material for highly efficient oxygen reduction reaction and Al-air battery. Electrochimica Acta, 2020, 341, 136066.	2.6	14
64	Hierarchical peony-like FeCo-NC with conductive network and highly active sites as efficient electrocatalyst for rechargeable Zn-air battery. Nano Research, 2020, 13, 1090-1099.	5.8	77
65	Recent Advances in Nonâ€Precious Metalâ€Based Electrodes for Alkaline Water Electrolysis. ChemNanoMat, 2020, 6, 336-355.	1.5	92
66	Confined local oxygen gas promotes electrochemical water oxidation to hydrogen peroxide. Nature Catalysis, 2020, 3, 125-134.	16.1	252
67	Common-Ion Effect Triggered Highly Sustained Seawater Electrolysis with Additional NaCl Production. Research, 2020, 2020, 2872141.	2.8	28
68	Porous Copper Foam Co-operation with Thiourea for Dendrite-free Lithium Metal Anode. Wuli Huaxue Xuebao/ Acta Physico - Chimica Sinica, 2020, .	2.2	2
69	Zn Doped NiMn-Layered Double Hydroxide for High Performance Ni–Zn Battery. Journal of the Electrochemical Society, 2020, 167, 160550.	1.3	4
70	An advanced zinc air battery with nanostructured superwetting electrodes. Energy Storage Materials, 2019, 17, 358-365.	9.5	25
71	Ultrathin atomic Mn-decorated formamide-converted N-doped carbon for efficient oxygen reduction reaction. Nanoscale, 2019, 11, 15900-15906.	2.8	43
72	Hierarchical cobalt oxide@Nickel-vanadium layer double hydroxide core/shell nanowire arrays with enhanced areal specific capacity for nickel–zinc batteries. Journal of Power Sources, 2019, 436, 226867.	4.0	48

#	Article	IF	CITATIONS
73	Dendriteâ€Free Lithium Deposition via a Superfilling Mechanism for Highâ€Performance Liâ€Metal Batteries. Advanced Materials, 2019, 31, e1903248.	11.1	106
74	Amorphous Ruthenium‣ulfide with Isolated Catalytic Sites for Pt‣ike Electrocatalytic Hydrogen Production Over Whole pH Range. Small, 2019, 15, e1904043.	5.2	71
75	Hydrogen Production: Amorphous Rutheniumâ€Sulfide with Isolated Catalytic Sites for Ptâ€Like Electrocatalytic Hydrogen Production Over Whole pH Range (Small 46/2019). Small, 2019, 15, 1970249.	5.2	0
76	Constructing Earthâ€abundant 3D Nanoarrays for Efficient Overall Water Splitting – A Review. ChemCatChem, 2019, 11, 1550-1575.	1.8	108
77	Superaerophilic copper nanowires for efficient and switchable CO <sub>2</sub> electroreduction. Nanoscale Horizons, 2019, 4, 490-494.	4.1	39
78	Activating Layered Double Hydroxide with Multivacancies by Memory Effect for Energy-Efficient Hydrogen Production at Neutral pH. ACS Energy Letters, 2019, 4, 1412-1418.	8.8	115
79	Engineering Interfacial Aerophilicity of Nickel-Embedded Nitrogen-Doped CNTs for Electrochemical CO <sub>2</sub> Reduction. ACS Applied Energy Materials, 2019, 2, 3991-3998.	2.5	23
80	Enhancing oxygen evolution reaction by cationic surfactants. Nano Research, 2019, 12, 2302-2306.	5.8	28
81	Synthesis and performance optimization of ultrathin two-dimensional CoFePt alloy materials <i>via in situ</i> topotactic conversion for the hydrogen evolution reaction. Journal of Materials Chemistry A, 2019, 7, 9517-9522.	5.2	17
82	Solar-driven, highly sustained splitting of seawater into hydrogen and oxygen fuels. Proceedings of the United States of America, 2019, 116, 6624-6629.	3.3	524
83	A general route <i>via</i> formamide condensation to prepare atomically dispersed metal–nitrogen–carbon electrocatalysts for energy technologies. Energy and Environmental Science, 2019, 12, 1317-1325.	15.6	290
84	Highly efficient and stable solar-powered desalination by tungsten carbide nanoarray film with sandwich wettability. Science Bulletin, 2019, 64, 391-399.	4.3	32
85	Boosting oxygen evolution of single-atomic ruthenium through electronic coupling with cobalt-iron layered double hydroxides. Nature Communications, 2019, 10, 1711.	5.8	446
86	An electrodeposition approach to metal/metal oxide heterostructures for active hydrogen evolution catalysts in near-neutral electrolytes. Nano Research, 2019, 12, 1431-1435.	5.8	31
87	An Entangled Cobalt–Nitrogen–Carbon Nanotube Array Electrode with Synergetic Confinement and Electrocatalysis of Polysulfides for Stable Li–S Batteries. ACS Applied Energy Materials, 2019, 2, 2904-2912.	2.5	28
88	Breaking the symmetry: Gradient in NiFe layered double hydroxide nanoarrays for efficient oxygen evolution. Nano Energy, 2019, 60, 661-666.	8.2	52
89	Electronic Structure Engineering of 2D Carbon Nanosheets by Evolutionary Nitrogen Modulation for Synergizing CO <sub>2</sub> Electroreduction. ACS Applied Energy Materials, 2019, 2, 3151-3159.	2.5	7
90	Recent Advances for MOFâ€Derived Carbonâ€Supported Singleâ€Atom Catalysts. Small Methods, 2019, 3, 1800471.	4.6	315

#	Article	IF	CITATIONS
91	Surface Restraint Synthesis of an Organic–Inorganic Hybrid Layer for Dendrite-Free Lithium Metal Anode. ACS Applied Materials & Interfaces, 2019, 11, 8717-8724.	4.0	39
92	NiFe Hydroxide Lattice Tensile Strain: Enhancement of Adsorption of Oxygenated Intermediates for Efficient Water Oxidation Catalysis. Angewandte Chemie, 2019, 131, 746-750.	1.6	55
93	Selectivity regulation of CO2 electroreduction through contact interface engineering on superwetting Cu nanoarray electrodes. Nano Research, 2019, 12, 345-349.	5.8	80
94	NiFe Hydroxide Lattice Tensile Strain: Enhancement of Adsorption of Oxygenated Intermediates for Efficient Water Oxidation Catalysis. Angewandte Chemie - International Edition, 2019, 58, 736-740.	7.2	335
95	Janus electrode with simultaneous management on gas and liquid transport for boosting oxygen reduction reaction. Nano Research, 2019, 12, 177-182.	5.8	43
96	Global Tudor‧N transgenic mice are protected from obesityâ€induced hepatic steatosis and insulin resistance. FASEB Journal, 2019, 33, 3731-3745.	0.2	4
97	Recent progress on earth abundant electrocatalysts for hydrogen evolution reaction (HER) in alkaline medium to achieve efficient water splitting – A review. Journal of Energy Chemistry, 2019, 34, 111-160.	7.1	323
98	Nitrogen-doped tungsten carbide nanoarray as an efficient bifunctional electrocatalyst for water splitting in acid. Nature Communications, 2018, 9, 924.	5.8	571
99	A highly-efficient oxygen evolution electrode based on defective nickel-iron layered double hydroxide. Science China Materials, 2018, 61, 939-947.	3.5	69
100	Oncoprotein Tudor-SN is a key determinant providing survival advantage under DNA damaging stress. Cell Death and Differentiation, 2018, 25, 1625-1637.	5.0	23
101	Tuning Electronic Structure of NiFe Layered Double Hydroxides with Vanadium Doping toward High Efficient Electrocatalytic Water Oxidation. Advanced Energy Materials, 2018, 8, 1703341.	10.2	505
102	Understanding the incorporating effect of Co2+/Co3+ in NiFe-layered double hydroxide for electrocatalytic oxygen evolution reaction. Journal of Catalysis, 2018, 358, 100-107.	3.1	194
103	Scalable fabrication of hierarchically porous N-doped carbon electrode materials for high-performance aqueous symmetric supercapacitor. Journal of Materials Science, 2018, 53, 5194-5203.	1.7	12
104	Density gradient ultracentrifugation for colloidal nanostructures separation and investigation. Science Bulletin, 2018, 63, 645-662.	4.3	35
105	Layered double hydroxides with atomic-scale defects for superior electrocatalysis. Nano Research, 2018, 11, 4524-4534.	5.8	130
106	Metal-organic framework-derived, Zn-doped porous carbon polyhedra with enhanced activity as bifunctional catalysts for rechargeable zinc-air batteries. Nano Research, 2018, 11, 163-173.	5.8	105
107	Singleâ€Crystalline Ultrathin Co <sub>3</sub> O <sub>4</sub> Nanosheets with Massive Vacancy Defects for Enhanced Electrocatalysis. Advanced Energy Materials, 2018, 8, 1701694.	10.2	451
108	Nanoporous Zn-doped Co3O4 sheets with single-unit-cell-wide lateral surfaces for efficient oxygen evolution and water splitting. Nano Energy, 2018, 44, 371-377.	8.2	138

#	Article	IF	CITATIONS
109	NiCoFeâ€Layered Double Hydroxides/Nâ€Doped Graphene Oxide Array Colloid Composite as an Efficient Bifunctional Catalyst for Oxygen Electrocatalytic Reactions. Advanced Energy Materials, 2018, 8, 1701905.	10.2	276
110	Fabricating Sulfur/Oxygen Coâ€Doped Crumpled Graphene for Highâ€Performance Oxygen Reduction Reaction Electrocatalysis. ChemElectroChem, 2018, 5, 242-246.	1.7	4
111	Co/CoP embedded in a hairy nitrogen-doped carbon polyhedron as an advanced tri-functional electrocatalyst. Materials Horizons, 2018, 5, 108-115.	6.4	184
112	Effects of redox-active interlayer anions on the oxygen evolution reactivity of NiFe-layered double hydroxide nanosheets. Nano Research, 2018, 11, 1358-1368.	5.8	134
113	Topotactic conversion of calcium carbide to highly crystalline few-layer graphene in water. Journal of Materials Chemistry A, 2018, 6, 23638-23643.	5.2	8
114	Polyvinylchloride-derived N, S co-doped carbon as an efficient sulfur host for high-performance Li–S batteries. RSC Advances, 2018, 8, 37811-37816.	1.7	10
115	Boosting oxygen reaction activity by coupling sulfides for high-performance rechargeable metal–air battery. Journal of Materials Chemistry A, 2018, 6, 21162-21166.	5.2	38
116	Microâ€∤Nanohoneycomb Solid Oxide Electrolysis Cell Anodes with Ultralarge Current Tolerance. Advanced Energy Materials, 2018, 8, 1802203.	10.2	40
117	Self-powered H2 production with bifunctional hydrazine as sole consumable. Nature Communications, 2018, 9, 4365.	5.8	178
118	Unlocking Bifunctional Electrocatalytic Activity for CO <sub>2</sub> Reduction Reaction by Win-Win Metal–Oxide Cooperation. ACS Energy Letters, 2018, 3, 2816-2822.	8.8	76
119	Flameâ€Engraved Nickel–Iron Layered Double Hydroxide Nanosheets for Boosting Oxygen Evolution Reactivity. Small Methods, 2018, 2, 1800083.	4.6	115
120	Activating basal plane in NiFe layered double hydroxide by Mn <sup>2+</sup> doping for efficient and durable oxygen evolution reaction. Nanoscale Horizons, 2018, 3, 532-537.	4.1	144
121	Systematic design of superaerophobic nanotube-array electrode comprised of transition-metal sulfides for overall water splitting. Nature Communications, 2018, 9, 2452.	5.8	431
122	Nanoseparation Using Density Gradient Ultracentrifugation. Springer Briefs in Molecular Science, 2018, , .	0.1	1
123	Aligned N-doped carbon nanotube bundles with interconnected hierarchical structure as an efficient bi-functional oxygen electrocatalyst. RSC Advances, 2018, 8, 26004-26010.	1.7	11
124	Recent progress on earth abundant electrocatalysts for oxygen evolution reaction (OER) in alkaline medium to achieve efficient water splitting $\hat{a} \in A$ review. Journal of Power Sources, 2018, 400, 31-68.	4.0	418
125	Plasma-activated Co3(PO4)2 nanosheet arrays with Co3+-Rich surfaces for overall water splitting. Journal of Power Sources, 2018, 400, 190-197.	4.0	86
126	Superwetting Electrodes for Gas-Involving Electrocatalysis. Accounts of Chemical Research, 2018, 51, 1590-1598.	7.6	411

#	Article	IF	CITATIONS
127	Introducing Fe <sup>2+</sup> into Nickel–Iron Layered Double Hydroxide: Local Structure Modulated Water Oxidation Activity. Angewandte Chemie, 2018, 130, 9536-9540.	1.6	86
128	Introducing Fe <sup>2+</sup> into Nickel–Iron Layered Double Hydroxide: Local Structure Modulated Water Oxidation Activity. Angewandte Chemie - International Edition, 2018, 57, 9392-9396.	7.2	284
129	Room-temperature rapid synthesis of metal-free doped carbon materials. Carbon, 2017, 115, 28-33.	5.4	18
130	Phosphorus oxoanion-intercalated layered double hydroxides for high-performance oxygen evolution. Nano Research, 2017, 10, 1732-1739.	5.8	139
131	Nickel–cobalt oxides supported on Co/N decorated graphene as an excellent bifunctional oxygen catalyst. Journal of Materials Chemistry A, 2017, 5, 5594-5600.	5.2	119
132	Regulating the spatial distribution of metal nanoparticles within metal-organic frameworks to enhance catalytic efficiency. Nature Communications, 2017, 8, 14429.	5.8	179
133	A two-volt aqueous supercapacitor from porous dehalogenated carbon. Journal of Materials Chemistry A, 2017, 5, 6734-6739.	5.2	23
134	Construction of Hierarchical Copperâ€Based Metal–Organic Framework Nanoarrays as Functional Structured Catalysts. ChemCatChem, 2017, 9, 1771-1775.	1.8	18
135	A promising energy storage system: rechargeable Ni–Zn battery. Rare Metals, 2017, 36, 381-396.	3.6	69
136	Thin sandwich graphene oxide@N-doped carbon composites for high-performance supercapacitors. RSC Advances, 2017, 7, 22071-22078.	1.7	6
137	Flexible Transparent Supercapacitors Based on Hierarchical Nanocomposite Films. ACS Applied Materials & Interfaces, 2017, 9, 17865-17871.	4.0	80
138	A flexible transparent colorimetric wrist strap sensor. Nanoscale, 2017, 9, 869-874.	2.8	104
139	Carbon coated Au/TiO2 mesoporous microspheres: a novel selective photocatalyst. Science China Materials, 2017, 60, 438-448.	3.5	25
140	Topotactic reduction of layered double hydroxides for atomically thick two-dimensional non-noble-metal alloy. Nano Research, 2017, 10, 2988-2997.	5.8	38
141	Multiâ€shelled Hollow Metal–Organic Frameworks. Angewandte Chemie - International Edition, 2017, 56, 5512-5516.	7.2	280
142	Innenrücktitelbild: Multiâ€shelled Hollow Metal–Organic Frameworks (Angew. Chem. 20/2017). Angewandte Chemie, 2017, 129, 5723-5723.	1.6	0
143	Multiâ€shelled Hollow Metal–Organic Frameworks. Angewandte Chemie, 2017, 129, 5604-5608.	1.6	45
144	Tuning the wettability of carbon nanotube arrays for efficient bifunctional catalysts and Zn–air batteries. Journal of Materials Chemistry A, 2017, 5, 7103-7110.	5.2	62

#	Article	IF	CITATIONS
145	Single Crystalline Ultrathin Nickel–Cobalt Alloy Nanosheets Array for Direct Hydrazine Fuel Cells. Advanced Science, 2017, 4, 1600179.	5.6	104
146	Efficient and stable electroreduction of CO <sub>2</sub> to CH <sub>4</sub> on CuS nanosheet arrays. Journal of Materials Chemistry A, 2017, 5, 20239-20243.	5.2	119
147	Superaerophobic Ultrathin Ni–Mo Alloy Nanosheet Array from In Situ Topotactic Reduction for Hydrogen Evolution Reaction. Small, 2017, 13, 1701648.	5.2	190
148	Interfacial dehalogenation-enabled hollow N-doped carbon network as bifunctional catalysts for rechargeable Zn-air battery. Electrochimica Acta, 2017, 247, 1044-1051.	2.6	19
149	3D Self‣upported Feâ€Đoped Ni <sub>2</sub> P Nanosheet Arrays as Bifunctional Catalysts for Overall Water Splitting. Advanced Functional Materials, 2017, 27, 1702513.	7.8	454
150	Polymer Dehalogenation-Enabled Fast Fabrication of N,S-Codoped Carbon Materials for Superior Supercapacitor and Deionization Applications. ACS Applied Materials & Interfaces, 2017, 9, 29753-29759.	4.0	81
151	Boosting the bifunctional electrocatalytic oxygen activities of CoO <sub>x</sub> nanoarrays with a porous N-doped carbon coating and their application in Zn–air batteries. Journal of Materials Chemistry A, 2017, 5, 17804-17810.	5.2	46
152	Cobaltâ€Embedded Nitrogenâ€Doped Carbon Nanotubes as Highâ€Performance Bifunctional Oxygen Catalysts. Energy Technology, 2017, 5, 1265-1271.	1.8	26
153	Superaerophobic RuO <sub>2</sub> â€Based Nanostructured Electrode for Highâ€Performance Chlorine Evolution Reaction. Small, 2017, 13, 1602240.	5.2	93
154	Investigation for the synthesis of hierarchical Co3O4@MnO2 nanoarrays materials and their application for supercapacitor. Journal of Materials Science: Materials in Electronics, 2017, 28, 1281-1287.	1.1	17
155	Sulfophenyl-Functionalized Reduced Graphene Oxide Networks on Electrospun 3D Scaffold for Ultrasensitive NO2 Gas Sensor. Sensors, 2017, 17, 2954.	2.1	18
156	Flexible Transparent Electronic Gas Sensors. Small, 2016, 12, 3748-3756.	5.2	234
157	Unconventional Carbon: Alkaline Dehalogenation of Polymers Yields Nâ€Doped Carbon Electrode for Highâ€Performance Capacitive Energy Storage. Advanced Functional Materials, 2016, 26, 3340-3348.	7.8	95
158	Superaerophilic Carbonâ€Nanotubeâ€Array Electrode for Highâ€Performance Oxygen Reduction Reaction. Advanced Materials, 2016, 28, 7155-7161.	11.1	231
159	Probing the seeded protocol for high-concentration preparation of silver nanowires. Nano Research, 2016, 9, 1532-1542.	5.8	25
160	ZnO-promoted dechlorination for hierarchically nanoporous carbon as superior oxygen reduction electrocatalyst. Nano Energy, 2016, 26, 241-247.	8.2	72
161	Hierarchical graphene–polyaniline nanocomposite films for high-performance flexible electronic gas sensors. Nanoscale, 2016, 8, 12073-12080.	2.8	132
162	Hierarchical mesoporous NiO nanoarrays with ultrahigh capacitance for aqueous hybrid supercapacitor. Nano Energy, 2016, 30, 831-839.	8.2	183

#	Article	IF	CITATIONS
163	Flexible Room-Temperature Gas Sensors of Nanocomposite Network-Coated Papers. ChemistrySelect, 2016, 1, 2816-2820.	0.7	10
164	Dehydrated layered double hydroxides: Alcohothermal synthesis and oxygen evolution activity. Nano Research, 2016, 9, 3152-3161.	5.8	30
165	Universal Parameter Optimization of Density Gradient Ultracentrifugation Using CdSe Nanoparticles as Tracing Agents. Analytical Chemistry, 2016, 88, 8495-8501.	3.2	11
166	Amorphous Co–Mo–S ultrathin films with low-temperature sulfurization as high-performance electrocatalysts for the hydrogen evolution reaction. Journal of Materials Chemistry A, 2016, 4, 13731-13735.	5.2	48
167	WO <sub>3</sub> @αâ€Fe <sub>2</sub> O <sub>3</sub> Heterojunction Arrays with Improved Photoelectrochemical Behavior for Neutral pH Water Splitting. ChemCatChem, 2016, 8, 2765-2770.	1.8	55
168	Synthesis of Ultrastable Ag Nanoplates/Polyethylenimine–Reduced Graphene Oxide and Its Application as a Versatile Electrochemical Sensor. Chemistry - A European Journal, 2016, 22, 10923-10929.	1.7	8
169	Wall-like hierarchical metal oxide nanosheet arrays grown on carbon cloth for excellent supercapacitor electrodes. Nanoscale, 2016, 8, 13273-13279.	2.8	144
170	Size Control Methods and Size-Dependent Properties of Graphene. , 2016, , 27-40.		0
171	Ternary NiCoP nanosheet arrays: An excellent bifunctional catalyst for alkaline overall water splitting. Nano Research, 2016, 9, 2251-2259.	5.8	342
172	N-doped crumpled graphene: bottom-up synthesis and its superior oxygen reduction performance. Science China Materials, 2016, 59, 337-347.	3.5	39
173	One‣tep Scalable Production of Co <sub>1â^'</sub> <i><sub>x</sub></i> S/Graphene Nanocomposite as Highâ€Performance Bifunctional Electrocatalyst. Particle and Particle Systems Characterization, 2016, 33, 569-575.	1.2	21
174	High-Performance Water Electrolysis System with Double Nanostructured Superaerophobic Electrodes. Small, 2016, 12, 2492-2498.	5.2	113
175	Binary nickel–iron nitride nanoarrays as bifunctional electrocatalysts for overall water splitting. Inorganic Chemistry Frontiers, 2016, 3, 630-634.	3.0	145
176	Ternary NiFeMn layered double hydroxides as highly-efficient oxygen evolution catalysts. Chemical Communications, 2016, 52, 908-911.	2.2	293
177	Singleâ€Crystalline Ultrathin Nickel Nanosheets Array from Inâ€Situ Topotactic Reduction for Active and Stable Electrocatalysis. Angewandte Chemie - International Edition, 2016, 55, 693-697.	7.2	225
178	Superior anti-CO poisoning capability: Au-decorated PtFe nanocatalysts for high-performance methanol oxidation. Chemical Communications, 2016, 52, 3903-3906.	2.2	57
179	A 3D porous Ni–Cu alloy film for high-performance hydrazine electrooxidation. Nanoscale, 2016, 8, 1479-1484.	2.8	74
180	An alternative pathway to water soluble functionalized graphene from the defluorination of graphite fluoride. Carbon, 2016, 96, 1022-1027.	5.4	21

#	Article	IF	CITATIONS
181	Hierarchical Co-based Porous Layered Double Hydroxide Arrays Derived via Alkali Etching for High-performance Supercapacitors. Scientific Reports, 2015, 5, 13082.	1.6	48
182	Superaerophobic Electrodes for Direct Hydrazine Fuel Cells. Advanced Materials, 2015, 27, 2361-2366.	11.1	232
183	Flexible Transparent Films Based on Nanocomposite Networks of Polyaniline and Carbon Nanotubes for Highâ€Performance Gas Sensing. Small, 2015, 11, 5409-5415.	5.2	225
184	Morphology and Phase Evolution of CoAl Layered Double Hydroxides in an Alkaline Environment with Enhanced Pseudocapacitive Performance. ChemElectroChem, 2015, 2, 679-683.	1.7	16
185	Healable, Transparent, Roomâ€Temperature Electronic Sensors Based on Carbon Nanotube Networkâ€Coated Polyelectrolyte Multilayers. Small, 2015, 11, 5807-5813.	5.2	151
186	Ag-Modified In2O3/ZnO Nanobundles with High Formaldehyde Gas-Sensing Performance. Sensors, 2015, 15, 20086-20096.	2.1	22
187	NiCo <sub>2</sub> O <sub>4</sub> @NiO hybrid arrays with improved electrochemical performance for pseudocapacitors. Journal of Materials Chemistry A, 2015, 3, 13900-13905.	5.2	147
188	Three-dimensional flower-like Co(OH)2 microspheres of nanoflakes/nanorods assembled on nickel foam as binder-free electrodes for High performance supercapacitors. Materials Letters, 2015, 158, 17-20.	1.3	19
189	Underâ€Water Superaerophobic Pineâ€Shaped Pt Nanoarray Electrode for Ultrahighâ€Performance Hydrogen Evolution. Advanced Functional Materials, 2015, 25, 1737-1744.	7.8	397
190	Nanoarray based "superaerophobic―surfaces for gas evolution reaction electrodes. Materials Horizons, 2015, 2, 294-298.	6.4	146
191	A metallic CoS <sub>2</sub> nanopyramid array grown on 3D carbon fiber paper as an excellent electrocatalyst for hydrogen evolution. Journal of Materials Chemistry A, 2015, 3, 6306-6310.	5.2	145
192	Development of hydrophilicity gradient ultracentrifugation method for photoluminescence investigation of separated non-sedimental carbon dots. Nano Research, 2015, 8, 2810-2821.	5.8	49
193	Amorphous Co-doped MoS <sub>2</sub> nanosheet coated metallic CoS <sub>2</sub> nanocubes as an excellent electrocatalyst for hydrogen evolution. Journal of Materials Chemistry A, 2015, 3, 15020-15023.	5.2	159
194	Rational design of graphene oxide and its hollow CoO composite for superior oxygen reduction reaction. Science China Materials, 2015, 58, 534-542.	3.5	30
195	A First-Principles Study of Oxygen Formation Over NiFe-Layered Double Hydroxides Surface. Catalysis Letters, 2015, 145, 1541-1548.	1.4	61
196	Adsolubilization of 2,4,6-trichlorophenol from aqueous solution by surfactant intercalated ZnAl layered double hydroxides. Chemical Engineering Journal, 2015, 279, 597-604.	6.6	36
197	Room-temperature synthetic NiFe layered double hydroxide with different anions intercalation as an excellent oxygen evolution catalyst. RSC Advances, 2015, 5, 55131-55135.	1.7	77
198	First-Principles Study of Oxygen Evolution Reaction on the Oxygen-Containing Species Covered Coll-Exposing Co3O4 (100) Surface. Catalysis Letters, 2015, 145, 1169-1176.	1.4	18

#	Article	IF	CITATIONS
199	Enhancement of capacitive deionization capacity of hierarchical porous carbon. Journal of Materials Chemistry A, 2015, 3, 12730-12737.	5.2	69
200	Trinary Layered Double Hydroxides as Highâ€Performance Bifunctional Materials for Oxygen Electrocatalysis. Advanced Energy Materials, 2015, 5, 1500245.	10.2	328
201	Separation of colloidal two dimensional materials by density gradient ultracentrifugation. Journal of Solid State Chemistry, 2015, 224, 120-126.	1.4	7
202	Controllable Assembly and Separation of Colloidal Nanoparticles through a Oneâ€Tube Synthesis Based on Density Gradient Centrifugation. Chemistry - A European Journal, 2015, 21, 7211-7216.	1.7	11
203	Selective removal of thiosulfate from thiocyanate-containing water by a three-dimensional structured adsorbent: a calcined NiAl-layered double hydroxide film. RSC Advances, 2015, 5, 87948-87955.	1.7	16
204	Single-crystalline dendritic bimetallic and multimetallic nanocubes. Chemical Science, 2015, 6, 7122-7129.	3.7	61
205	Residual metals present in "metal-free―N-doped carbons. Chemical Communications, 2015, 51, 15585-15587.	2.2	11
206	Three-dimensional porous superaerophobic nickel nanoflower electrodes for high-performance hydrazine oxidation. Nano Research, 2015, 8, 3365-3371.	5.8	70
207	Hierarchical nanoarray materials for advanced nickel–zinc batteries. Inorganic Chemistry Frontiers, 2015, 2, 184-187.	3.0	88
208	Hierarchically porous indium oxide nanolamellas with ten-parts-per-billion-level formaldehyde-sensing performance. Sensors and Actuators B: Chemical, 2015, 206, 714-720.	4.0	31
209	Synthesis of hierarchical porous N-doped sandwich-type carbon composites as high-performance supercapacitor electrodes. Journal of Materials Chemistry A, 2015, 3, 3667-3675.	5.2	73
210	Ultrathin branched PtFe and PtRuFe nanodendrites with enhanced electrocatalytic activity. Journal of Materials Chemistry A, 2015, 3, 1182-1187.	5.2	65
211	Transparent Conducting Films of Hierarchically Nanostructured Polyaniline Networks on Flexible Substrates for High-Performance Gas Sensors. Small, 2015, 11, 306-310.	5.2	133
212	Nucleic acid from beans extracted by ethanediamine magnetic particles. Journal of Food Science and Technology, 2015, 52, 1784-1789.	1.4	2
213	NiCoFe spinel-type oxide nanosheet arrays derived from layered double hydroxides as structured catalysts. RSC Advances, 2014, 4, 57804-57809.	1.7	15
214	Hierarchical ultrathin rolled-up Co(OH)(CO3)0.5films assembled on Ni0.25Co0.75Sxnanosheets for enhanced supercapacitive performance. RSC Advances, 2014, 4, 57458-57462.	1.7	4
215	Effect of internal noise on the oscillation of N2O decomposition over Cu-ZSM-5 zeolites using a stochastic description. Journal of Chemical Physics, 2014, 140, 044715.	1.2	1
216	Au/NiCo <sub>2</sub> O <sub>4</sub> Arrays with High Activity for Water Oxidation. ChemCatChem, 2014, 6, 2501-2506.	1.8	60

#	Article	IF	CITATIONS
217	Transition metal oxides/hydroxides nanoarrays for aqueous electrochemical energy storage systems. Science China Materials, 2014, 57, 59-69.	3.5	42
218	Ultrahigh Hydrogen Evolution Performance of Underâ€Water "Superaerophobic―MoS <sub>2</sub> Nanostructured Electrodes. Advanced Materials, 2014, 26, 2683-2687.	11.1	775
219	Three-dimensional NiAl-mixed metal oxide film: preparation and capacitive deionization performances. RSC Advances, 2014, 4, 41642-41648.	1.7	25
220	Highly Crystallized Cubic Cattierite CoS 2 for Electrochemically Hydrogen Evolution over Wide pH Range from 0 to 14. Electrochimica Acta, 2014, 148, 170-174.	2.6	80
221	Solvent switching and purification of colloidal nanoparticles through water/oil Interfaces within a density gradient. Nano Research, 2014, 7, 1670-1679.	5.8	8
222	Green sacrificial template fabrication of hierarchical MoO3 nanostructures. CrystEngComm, 2014, 16, 3935.	1.3	13
223	Asymmetric hetero-assembly of colloidal nanoparticles through "crash reaction―in a centrifugal field. Dalton Transactions, 2014, 43, 5994-5997.	1.6	7
224	Shape evolution of Au nanoring@Ag core–shell nanostructures: diversity from a sole seed. Dalton Transactions, 2014, 43, 12495.	1.6	13
225	A novel structured catalyst: gold supported on thin bimetallic (Ni, Co) carbonate hydroxide nanosheet arrays. Journal of Materials Chemistry A, 2014, 2, 8230-8235.	5.2	9
226	Urchin-like TiO <sub>2</sub> @C core–shell microspheres: coupled synthesis and lithium-ion battery applications. Physical Chemistry Chemical Physics, 2014, 16, 8808-8811.	1.3	25
227	One-dimensional copper oxide nanotube arrays: biosensors for glucose detection. RSC Advances, 2014, 4, 1449-1455.	1.7	59
228	A hierarchical Ni–Co–O@Ni–Co–S nanoarray as an advanced oxygen evolution reaction electrode. Physical Chemistry Chemical Physics, 2014, 16, 20402-20405.	1.3	54
229	Ultrathin Dendritic Pt <sub>3</sub> Cu Triangular Pyramid Caps with Enhanced Electrocatalytic Activity. ACS Applied Materials & Interfaces, 2014, 6, 17748-17752.	4.0	69
230	Hierarchical NiAl Layered Double Hydroxide/Multiwalled Carbon Nanotube/Nickel Foam Electrodes with Excellent Pseudocapacitive Properties. ACS Applied Materials & Interfaces, 2014, 6, 16304-16311.	4.0	112
231	Porous MoO <sub>3</sub> Film as a Highâ€Performance Anode Material for Lithiumâ€Ion Batteries. ChemElectroChem, 2014, 1, 1476-1479.	1.7	26
232	A 3D Nanoporous Ni-Mo Electrocatalyst with Negligible Overpotential for Alkaline Hydrogen Evolution. ChemElectroChem, 2014, 1, 1089-1089.	1.7	1
233	Hierarchical Zn <i><sub>x</sub></i> Co <sub>3–<i>x</i></sub> O <sub>4</sub> Nanoarrays with High Activity for Electrocatalytic Oxygen Evolution. Chemistry of Materials, 2014, 26, 1889-1895.	3.2	401
234	Solvothermal synthesis of FeCo nanoparticles for magneto-controllable biocatalysis. RSC Advances, 2014, 4, 11136-11141.	1.7	9

#	Article	IF	CITATIONS
235	High-performance aqueous battery with double hierarchical nanoarrays. Nano Energy, 2014, 10, 229-234.	8.2	24
236	Three-dimensional NiFe layered double hydroxide film for high-efficiency oxygen evolution reaction. Chemical Communications, 2014, 50, 6479-6482.	2.2	776
237	A 3D Nanoporous Ni–Mo Electrocatalyst with Negligible Overpotential for Alkaline Hydrogen Evolution. ChemElectroChem, 2014, 1, 1138-1144.	1.7	113
238	Electrochemical tuning of layered lithium transition metal oxides for improvement of oxygen evolution reaction. Nature Communications, 2014, 5, 4345.	5.8	411
239	Bottom-Up Assembly of Hydrophobic Nanocrystals and Graphene Nanosheets into Mesoporous Nanocomposites. Langmuir, 2014, 30, 4434-4440.	1.6	8
240	Highly stable Ag–Au nanoplates and nanoframes for two-photon luminescence. RSC Advances, 2014, 4, 35263.	1.7	14
241	Hierarchical construction of an ultrathin layered double hydroxide nanoarray for highly-efficient oxygen evolution reaction. Nanoscale, 2014, 6, 11789-11794.	2.8	169
242	Promoted Oxygen Reduction Activity of Ag/Reduced Graphene Oxide by Incorporated CoOx. Electrochimica Acta, 2014, 132, 136-141.	2.6	13
243	Hierarchical construction of core–shell metal oxide nanoarrays with ultrahigh areal capacitance. Nano Energy, 2014, 7, 170-178.	8.2	111
244	A Deep Investigation of the Thermal Decomposition Process of Supported Silver Catalysts. Bulletin of the Korean Chemical Society, 2014, 35, 1832-1836.	1.0	5
245	Syntheses and biological activity of chalcones-imidazole derivatives. Research on Chemical Intermediates, 2013, 39, 1037-1048.	1.3	20
246	Synthesis Mechanism Study of Layered Double Hydroxides Based on Nanoseparation. Inorganic Chemistry, 2013, 52, 8694-8698.	1.9	24
247	Separation and phase transition investigation of Yb3+/Er3+ co-doped NaYF4 nanoparticles. Dalton Transactions, 2013, 42, 13315.	1.6	10
248	α-Fe2O3 nanorod arrays for bioanalytical applications: nitrite and hydrogen peroxide detection. RSC Advances, 2013, 3, 8489.	1.7	21
249	In situ fabrication of porous MoS2 thin-films as high-performance catalysts for electrochemical hydrogen evolution. Chemical Communications, 2013, 49, 7516.	2.2	120
250	Metal oxide and hydroxide nanoarrays: Hydrothermal synthesis and applications as supercapacitors and nanocatalysts. Progress in Natural Science: Materials International, 2013, 23, 351-366.	1.8	176
251	V2O5 nanostructure arrays: controllable synthesis and performance as cathodes for lithium ion batteries. RSC Advances, 2013, 3, 19937.	1.7	14
252	General synthesis and self-assembly of lanthanide orthovanadate nanorod arrays. CrystEngComm, 2013, 15, 10230.	1.3	20

#	Article	IF	CITATIONS
253	Highly controlled bifunctional Ag@rubrene core–shell nanostructures: surface-enhanced fluorescence and Raman scattering. Journal of Materials Chemistry C, 2013, 1, 4146.	2.7	12
254	NiTi layered double hydroxide thin films for advanced pseudocapacitor electrodes. Journal of Materials Chemistry A, 2013, 1, 10655.	5.2	70
255	Ultrathin Co3O4 nanosheet arrays with high supercapacitive performance. Scientific Reports, 2013, 3, 3537.	1.6	177
256	The isothermal oscillations and fluctuation-driven oscillations of N2O decomposition over Cu-ZSM-5 zeolites. Chemical Physics Letters, 2013, 584, 195-199.	1.2	2
257	Effect of synthesis method on selective adsorption of thiosulfate by calcined MgAl-layered double hydroxides. Chemical Engineering Journal, 2013, 232, 510-518.	6.6	23
258	Mesoporous assembled SnO2 nanospheres: Controlled synthesis, structural analysis and ethanol sensing investigation. Sensors and Actuators B: Chemical, 2013, 181, 629-636.	4.0	21
259	Ag@zinc–tetraphenylporphyrin core–shell nanostructures with unusual thickness-tunable fluorescence. Chemical Communications, 2013, 49, 3513.	2.2	11
260	One-step scalable preparation of N-doped nanoporous carbon as a high-performance electrocatalyst for the oxygen reduction reaction. Nano Research, 2013, 6, 293-301.	5.8	142
261	Hierarchical Ni0.25Co0.75(OH)2 nanoarrays for a high-performance supercapacitor electrode prepared by an in situ conversion process. Journal of Materials Chemistry A, 2013, 1, 8327.	5.2	74
262	Size-control of Au-Ni Heteronanostructure. Acta Chimica Sinica, 2013, 71, 20130907.	0.5	0
263	Ligand-manipulated selective transformations of Au–Ni bimetallic heteronanostructures in an organic medium. Chemical Communications, 2012, 48, 6963.	2.2	14
264	Sea urchin-like Ag–α-Fe2O3 nanocomposite microspheres: synthesis and gas sensing applications. Journal of Materials Chemistry, 2012, 22, 7232.	6.7	85
265	A process-analysis microsystem based on density gradient centrifugation and its application in the study of the galvanic replacement mechanism of Ag nanoplates with HAuCl4. Chemical Communications, 2012, 48, 7241.	2.2	27
266	One-pot synthesis and catalyst support application of mesoporous N-doped carbonaceous materials. Journal of Materials Chemistry, 2012, 22, 12149.	6.7	33
267	Hierarchical cobalt iron oxide nanoarrays as structured catalysts. Chemical Communications, 2012, 48, 3379.	2.2	61
268	Ultrashort Single-Walled Carbon Nanotubes: Density Gradient Separation, Optical Property, and Mathematical Modeling Study. Journal of Physical Chemistry C, 2012, 116, 24770-24776.	1.5	18
269	Understanding the "Tailoring Synthesis―of CdS Nanorods by O <sub>2</sub> . Inorganic Chemistry, 2012, 51, 1302-1308.	1.9	16
270	Control of Surface Defects and Agglomeration Mechanism of Layered Double Hydroxide Nanoparticles. Industrial & Engineering Chemistry Research, 2012, 51, 4215-4221.	1.8	35

#	Article	IF	CITATIONS
271	Extracting genomic DNA of foodstuff by polyamidoamine (PAMAM)–magnetite nanoparticles. Talanta, 2012, 93, 166-171.	2.9	16
272	Preparation of Multiâ€Metal Oxide Hollow Sphere Using Layered Double Hydroxide Precursors. Chinese Journal of Chemistry, 2012, 30, 2183-2188.	2.6	13
273	High pseudocapacitive cobalt carbonate hydroxide films derived from CoAl layered double hydroxides. Nanoscale, 2012, 4, 3640.	2.8	144
274	Hierarchical Co <sub>3</sub> O <sub>4</sub> nanosheet@nanowire arrays with enhanced pseudocapacitive performance. RSC Advances, 2012, 2, 1663-1668.	1.7	125
275	One-pot solvothermal method to prepare functionalized Fe3O4 nanoparticles for bioseparation. Journal of Materials Research, 2012, 27, 1006-1013.	1.2	17
276	Hierarchical Co3O4@Ni-Co-O supercapacitor electrodes with ultrahigh specific capacitance per area. Nano Research, 2012, 5, 369-378.	5.8	156
277	Mesoporous Au/TiO <sub>2</sub> Nanocomposite Microspheres for Visibleâ€Light Photocatalysis. Chemistry - A European Journal, 2012, 18, 5361-5366.	1.7	50
278	Beta-phased Ni(OH)2 nanowall film with reversible capacitance higher than theoretical Faradic capacitance. Chemical Communications, 2011, 47, 9651.	2.2	261
279	Mg/Al-CO3 layered double hydroxide nanorings. Journal of Materials Chemistry, 2011, 21, 14741.	6.7	29
280	Titanate nanosheets and nanotubes: alkalinity manipulated synthesis and catalyst support application. Journal of Materials Chemistry, 2011, 21, 277-282.	6.7	33
281	Adsorption Behavior of Thiophene from Aqueous Solution on Carbonate- and Dodecylsulfate-Intercalated ZnAl Layered Double Hydroxides. Industrial & Engineering Chemistry Research, 2011, 50, 10253-10258.	1.8	27
282	Experimental and Mathematical Modeling Studies of the Separation of Zinc Blende and Wurtzite Phases of CdS Nanorods by Density Gradient Ultracentrifugation. ACS Nano, 2011, 5, 3242-3249.	7.3	35
283	Crystal plane effect of Fe2O3 with various morphologies on CO catalytic oxidation. Catalysis Communications, 2011, 12, 530-534.	1.6	106
284	Evaluation Criteria for Reduced Graphene Oxide. Journal of Physical Chemistry C, 2011, 115, 11327-11335.	1.5	451
285	Nanoseparation-inspired manipulation of the synthesis of CdS nanorods. Nano Research, 2011, 4, 226-232.	5.8	18
286	Stable ultrahigh specific capacitance of NiO nanorod arrays. Nano Research, 2011, 4, 658-665.	5.8	165
287	Separation of gold nanorods using density gradient ultracentrifugation. Nano Research, 2011, 4, 723-728.	5.8	29
288	Co-production of high quality NH4SCN and sulfur slow release agent from industrial effluent using calcined MgAl–hydrotalcite. Chemical Engineering Journal, 2011, 169, 151-156.	6.6	18

#	Article	IF	CITATIONS
289	Derivated titanate nanotubes and their hydrogen storage properties. Frontiers of Chemistry in China: Selected Publications From Chinese Universities, 2010, 5, 71-75.	0.4	2
290	Cerium Vanadate Nanorod Arrays from Ionic Chelatorâ€Mediated Selfâ€Assembly. Angewandte Chemie - International Edition, 2010, 49, 3492-3495.	7.2	48
291	Knowledge Dissemination on Community Networks. , 2010, , .		0
292	Notice of Retraction: How to Use the Brokerage Roles of Innovation Networks Efficiently. , 2010, , .		0
293	Monodisperse Chemically Modified Graphene Obtained by Density Gradient Ultracentrifugal Rate Separation. ACS Nano, 2010, 4, 3381-3389.	7.3	193
294	Graphene in Mice: Ultrahigh In Vivo Tumor Uptake and Efficient Photothermal Therapy. Nano Letters, 2010, 10, 3318-3323.	4.5	2,213
295	Cooperative Effect of Solvent in the Neutral Hydration of Ketenimine: An ab Initio Study Using the Hybrid Cluster/Continuum Model. Journal of Physical Chemistry A, 2010, 114, 595-602.	1.1	25
296	Rapid Separation and Purification of Nanoparticles in Organic Density Gradients. Journal of the American Chemical Society, 2010, 132, 2333-2337.	6.6	166
297	Separation of Nanoparticles in a Density Gradient: FeCo@C and Gold Nanocrystals. Angewandte Chemie - International Edition, 2009, 48, 939-942.	7.2	136
298	Quantum interference effect in single disordered silver nanowires. Physics Letters, Section A: General, Atomic and Solid State Physics, 2009, 373, 1181-1184.	0.9	2
299	Exploring the Reactivity Trends in the E2 and S <sub>N</sub> 2 Reactions of X <sup>â<sup>-</sup>'</sup> + CH <sub>3</sub> CH <sub>2</sub> CI (X = F, Cl, Br, HO, HS, HSe, NH <sub>2</sub> PH <sub>2</sub> ,) Tj ETQq1 1 Theory and Computation, 2009, 5, 1597-1606.	0,784314 2.3	+ rgβT /Overl
300	Nano-graphene oxide for cellular imaging and drug delivery. Nano Research, 2008, 1, 203-212.	5.8	3,043
301	Synthesis of Ultrasmall Ferromagnetic Face entered Tetragonal FePt–Graphite Core–Shell Nanocrystals. Small, 2008, 4, 1968-1971.	5.2	29
302	Highly conducting graphene sheets and Langmuir–Blodgett films. Nature Nanotechnology, 2008, 3, 538-542.	15.6	1,901
303	A pilot toxicology study of single-walled carbon nanotubes in a small sample of mice. Nature Nanotechnology, 2008, 3, 216-221.	15.6	705
304	PEGylated Nanographene Oxide for Delivery of Water-Insoluble Cancer Drugs. Journal of the American Chemical Society, 2008, 130, 10876-10877.	6.6	3,344
305	Optical Properties of Ultrashort Semiconducting Single-Walled Carbon Nanotube Capsules Down to Sub-10 nm. Journal of the American Chemical Society, 2008, 130, 6551-6555.	6.6	142
306	Supramolecular Chemistry on Water-Soluble Carbon Nanotubes for Drug Loading and Delivery. ACS Nano, 2007, 1, 50-56.	7.3	1,290

#	Article	IF	CITATIONS
307	Noncovalent Functionalization of Carbon Nanotubes by Fluoresceinâ^'Polyethylene Glycol:Â Supramolecular Conjugates with pH-Dependent Absorbance and Fluorescence. Journal of the American Chemical Society, 2007, 129, 2448-2449.	6.6	288
308	Langmuirâ^'Blodgett Assembly of Densely Aligned Single-Walled Carbon Nanotubes from Bulk Materials. Journal of the American Chemical Society, 2007, 129, 4890-4891.	6.6	373
309	In vivo biodistribution and highly efficient tumour targeting of carbon nanotubes in mice. Nature Nanotechnology, 2007, 2, 47-52.	15.6	1,384
310	Oxides@C Coreâ^'Shell Nanostructures:  One-Pot Synthesis, Rational Conversion, and Li Storage Property. Chemistry of Materials, 2006, 18, 3486-3494.	3.2	226
311	FeCo/graphitic-shell nanocrystals as advanced magnetic-resonance-imaging and near-infrared agents. Nature Materials, 2006, 5, 971-976.	13.3	807
312	Use of Carbonaceous Polysaccharide Microspheres as Templates for Fabricating Metal Oxide Hollow Spheres. Chemistry - A European Journal, 2006, 12, 2039-2047.	1.7	426
313	Hollow carbonaceous capsules from glucose solution. Journal of Colloid and Interface Science, 2005, 291, 7-12.	5.0	137
314	Enhanced catalytic activity of ceria nanorods from well-defined reactive crystal planes. Journal of Catalysis, 2005, 229, 206-212.	3.1	1,010
315	Synthesis of red-luminescent Eu3+-doped lanthanides compounds hollow spheres. Materials Research Bulletin, 2005, 40, 911-919.	2.7	38
316	Crystal Structures, Anisotropic Growth, and Optical Properties: Controlled Synthesis of Lanthanide Orthophosphate One-Dimensional Nanomaterials. Chemistry - A European Journal, 2005, 11, 2183-2195.	1.7	215
317	Favorable synergetic effects between CuO and the reactive planes of ceria nanorods. Catalysis Letters, 2005, 101, 169-173.	1.4	62
318	Ag@C Core/Shell Structured Nanoparticles:Â Controlled Synthesis, Characterization, and Assembly. Langmuir, 2005, 21, 6019-6024.	1.6	202
319	Surface Enhanced Raman Scattering Effects of Silver Colloids with Different Shapes. Journal of Physical Chemistry B, 2005, 109, 12544-12548.	1.2	359
320	Colloidal Carbon Spheres and Their Core/Shell Structures with Noble-Metal Nanoparticles. Angewandte Chemie - International Edition, 2004, 43, 597-601.	7.2	2,000
321	Ga2O3 and GaN Semiconductor Hollow Spheres. Angewandte Chemie - International Edition, 2004, 43, 3827-3831.	7.2	509
322	Highly Sensitive WO3 Hollow-Sphere Gas Sensors. Inorganic Chemistry, 2004, 43, 5442-5449.	1.9	565
323	Nanowires and Nanotubes of Complex Oxides. , 2003, , 173-190.		8
324	Catalytic growth of ZnO nanotubes. Materials Chemistry and Physics, 2003, 82, 997-1001.	2.0	142

#	Article	IF	CITATIONS
325	Self-organized growth of ZnO single crystal columns array. Materials Chemistry and Physics, 2003, 80, 366-370.	2.0	21
326	Synthesis and Characterization of Ion-Exchangeable Titanate Nanotubes. Chemistry - A European Journal, 2003, 9, 2229-2238.	1.7	895
327	Size-controllable luminescent single crystal CaF2 nanocubesElectronic supplementary information (ESI) available: two TEM images and two PL spectra. See http://www.rsc.org/suppdata/cc/b3/b303614f/. Chemical Communications, 2003, , 1768.	2.2	102
328	Large-Scale Synthesis of Sodium and Potassium Titanate Nanobelts. Inorganic Chemistry, 2002, 41, 4996-4998.	1.9	114
329	Structure-Directing Coordination Template Effect of Ethylenediamine in Formations of ZnS and ZnSe Nanocrystallites via Solvothermal Route. Inorganic Chemistry, 2002, 41, 869-873.	1.9	293
330	Self-Assembling Vanadium Oxide Nanotubes by Organic Molecular Templates. Inorganic Chemistry, 2002, 41, 4524-4530.	1.9	140
331	Formation of rod-like Mg(OH)2 nanocrystallites under hydrothermal conditions and the conversion to MgO nanorods by thermal dehydration. Materials Chemistry and Physics, 2002, 76, 119-122.	2.0	107
332	Evaporation growth of multipod ZnO whiskers assisted by a Cu2+ etching technique. Journal of Crystal Growth, 2002, 244, 218-223.	0.7	20
333	Bismuth Nanotubes:Â A Rational Low-Temperature Synthetic Route. Journal of the American Chemical Society, 2001, 123, 9904-9905.	6.6	481
334	Surfactant-assisted hydrothermal synthesis of hydroxyapatite nanorods. Solid State Sciences, 2001, 3, 633-637.	0.8	183
335	Converting Polyvinyl Chloride Plastic Wastes to Carbonaceous Materials via Room-Temperature Dehalogenation for High-Performance Supercapacitor. ACS Applied Energy Materials, 0, , .	2.5	9
336	Solvent Recyclable Synthesis of Nitrogenâ€Rich Nanotubes with Embedded CoFe Nanoparticles for Electrochemical Oxygenâ€Involving Reactions. Energy Technology, 0, , 2100957.	1.8	1